Real-time chirp diagnostic for ultrashort laser pulses

Toshiyuki Hirayama and Mansoor Sheik-Bahae

Department of Physics and Astronomy, University of New Mexico, Albuquerque, New Mexico 87131

Received October 9, 2001

Using a real-time Fourier-transform algorithm, we present a simple technique for measuring the chirp of femtosecond laser pulses. We demonstrate significantly enhanced sensitivity compared with standard autocorrelation measurements. © 2002 Optical Society of America

OCIS codes: 320.7100, 140.7090, 190.7110.

The remarkable progress achieved in the generation of ultrashort laser pulses has led to the development of reliable systems for industrial as well as research applications. Many applications demand high spectral and temporal purity of the laser pulses. This requirement has driven the development of elegant techniques for reconstruction of the complex electric field from a combination of autocorrelation and spectral data.[1–4] These measurements give details of the temporal amplitude and phase but are computationally intensive and involve elaborate experimental setups. In many applications, however, exact knowledge of the complex electric field is not necessary, provided that the pulse width can be determined and the phase distortions (i.e., chirp) can be minimized. In principle, both tasks can be performed in real time by interferometric autocorrelation (IAC) measurements.[5,6] Here we describe a modification to the IAC method that makes it much more sensitive to temporal chirp. This technique is simple and ideal for monitoring mode-locked laser pulses while performing real-time dispersion control to minimize the temporal phase distortions. We call this technique modified-spectrum autointerferometric correlation, or MOSAIC. We present an analysis of MOSAIC and demonstrate the principle experimentally by measuring the chirp of femtosecond Ti:sapphire laser pulses.

Assuming that the laser pulse has an irradiance temporal profile $f(t)$, the incident electric field is given by $E(t) = f^{1/2}(t)\cos[\omega t + \varphi(t)]$, where $\varphi(t)$ denotes the temporal chirp. In second-order IAC experiments (e.g., use of second-harmonic generation, two-photon absorption, or the Kerr effect), the detected signal (assuming a balanced interferometer) is given by[5,6]

$$S_{\mathrm{IAC}}(\tau) = 1 + 2\int f(t)f(t+\tau)\mathrm{d}\tau + \int f(t)f(t+\tau)\cos(2\omega\tau + 2\Delta\phi)\mathrm{d}t + 2\int f^{1/2}(t)f^{3/2}(t+\tau)\cos(\omega\tau + \Delta\phi)\mathrm{d}t + 2\int f^{3/2}(t)f^{1/2}(t+\tau)\cos(\omega\tau + \Delta\phi)\mathrm{d}t, \quad (1)$$

where $\Delta\phi(t,\tau) = \phi(t+\tau) - \phi(t)$ and $\int f(t)\mathrm{d}t = 1$. In Eq. (1), the first integral represents the intensity autocorrelation whereas the remaining integrals are interferometric terms that contain information about the phase (i.e., chirp) of the laser pulse. Figure 1 (right) is a calculated IAC trace for $f(t) \propto \mathrm{sech}^2(t/t_p)$ with linear chirp $[\phi = a(t/t_p)^2]$. IAC traces are often used to determine the pulse duration as well as the presence (or absence) of phase distortion. Visual interpretation of pulse chirp from an IAC trace, however, can be subjective and ambiguous. We show that simple transformation of an IAC to a MOSAIC representation can substantially reduce this problem. Equation (1) reveals there are three main spectral components of the IAC signal, centered at frequencies 0, ω, and 2ω. We obtain the MOSAIC by modifying the IAC spectrum as follows: the ω terms are eliminated, the 2ω term is amplified by a factor of 2, and the intensity autocorrelation term is unchanged. This spectral modification gives the time-domain MOSAIC signal:

$$S_{\mathrm{MOSAIC}}(\tau) = 1 + 2\int f(t)f(t+\tau)\mathrm{d}t + 2\int f(t)f(t+\tau)\cos(2\omega\tau + 2\Delta\phi)\mathrm{d}t. \quad (2)$$

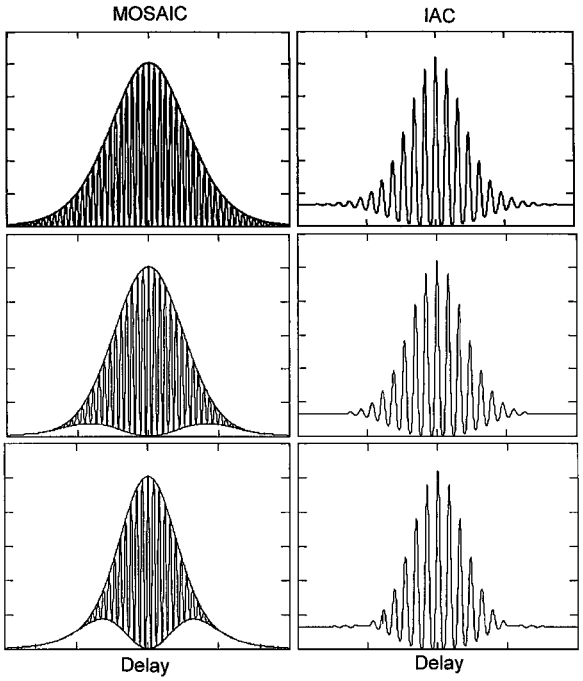

Fig. 1. Calculated autocorrelation traces corresponding to IAC and MOSAIC for various degrees of linear chirp obtained when we set $a = 0$ (top), $a = 0.15$ (middle), and $a = 0.25$ (bottom).

0146-9592/02/100860-03$15.00/0

This spectral modification was originally proposed as a method to eliminate the linear autocorrelation term (also at ω) for Kerr-lens autocorrelation measurements.[7] A similar filtering technique has also been used in ultrafast characterization of nonlinear susceptibilities.[8] The MOSAIC results that we calculated using Eq. (2) are plotted in Fig. 1 (left) for the same linear chirp function assumed for the IAC trace (right). The envelopes of the minima and maxima of the MOSAIC traces are also shown in Fig. 1 (left). The important property of the MOSAIC signal is that, with no chirp [$\phi(t) = 0$], the fringe visibility has an easily identified flat minimum. Compared with the IAC, assessment of frequency chirp is much clearer. Another advantage of this filtering scheme is that the normalized MOSAIC signal is insensitive to the relative intensity in the two arms of the interferometer; i.e., the measurements do not require an intensity-balanced interferometer.

These effects are demonstrated experimentally. We used a self-mode-locked Ti:sapphire laser pumped by a doubled Nd:YVO_4 laser (Coherent Verdi) that produced pulses with a duration ≈60 fs (FWHM) at 80 MHz and with a center wavelength $\lambda \approx 800$ nm. The chirp of the pulses was controlled by multipass propagation through a 6-mm-thick fused-silica window and to a lesser extent by the position of the intracavity prisms. Autocorrelation traces were obtained with a rapid-scan Michelson interferometer. Second-order correlation was obtained with a two-photon absorption-induced photocurrent in a green LED.[9] The IAC traces were monitored on a digital oscilloscope (Tektronix TDS 520D) and read into a computer equipped with Labview software. We obtained similar results by acquiring the data directly with an oscilloscope board (National Instruments NI5102), which is more economical and compact. We converted IAC traces into MOSAIC waveforms, using a fast Fourier-transform algorithm. The bandpass filter functions were taken as rectangular functions centered at ω and 2ω having bandwidths of ω. The final results can be displayed in real time for rapid-scan autocorrelations. Figure 2 compares IAC and MOSAIC traces for various amounts of chirp. Consistent with the calculations of Fig. 1, the MOSAIC traces are far more sensitive to chirp than the IAC traces, especially for low chirp. The enhanced sensitivity is due primarily to the twofold amplification of the interferometric term in Eq. (2). We can further analyze this by expanding the cosine term in Eq. (2) to derive an expression for the fringe visibility by use of the standard textbook procedure[10]:

$$S_{\mathrm{MOSAIC}}(\tau) = g(\tau) + [g_s{}^2(\tau) + g_c{}^2(\tau)]^{1/2} \times \cos[2\omega\tau + \Phi(\tau)], \quad (3)$$

where $g(\tau) = \int f(t)f(t+\tau)\mathrm{d}t$ is the intensity autocorrelation,

$$g_s(\tau) = \int f(t)f(t+\tau)\sin(2\Delta\phi)\mathrm{d}t,$$

$$g_c(\tau) = \int f(t)f(t+\tau)\cos(2\Delta\phi)\mathrm{d}t$$

are the sine and cosine intensity autocorrelations, respectively, and $\Phi(\tau) = -\tan^{-1}(g_s/g_c)$. The lower bound (minima envelope) of the MOSAIC trace is therefore given by

$$S^{\min}_{\mathrm{MOSAIC}}(\tau) = g(\tau) - [g_s{}^2(\tau) + g_c{}^2(\tau)]^{1/2}. \quad (4)$$

The peak of this envelope is seen to be a good measure of the pulse chirp. Normalized to the maximum of the MOSAIC signal [i.e., $2g(0)$], this quantity (here called the MOSAIC peak) is plotted in Fig. 3 versus the normalized mean chirp parameter [defined as $t_p \int f(t)|\mathrm{d}\phi/\mathrm{d}t|\mathrm{d}t / \int f(t)\mathrm{d}t$] for various orders of chirp of a sech^2 pulse, assuming a general time-dependent phase $\phi(t)$ that varies as either $a(t/t_p)^2$, $b(t/t_p)^3$ or $c(t/t_p)^4$. We should also address the case, often encountered in practice, in which two or more higher orders of chirp are simultaneously present in the laser pulse [e.g., when $\phi(t) = a(t/t_p)^2 + b(t/t_p)^3 + c(t/t_p)^4$]. More specifically, it is useful to know whether minimization of the MOSAIC peak can still correspond to the minimum of the mean chirp when two partially compensating chirp orders (such as first and third orders of opposite signs) are present in the pulse. The contour plots in Fig. 4 show the calculated mean chirp (left) and the MOSAIC peak (right) as the first- and

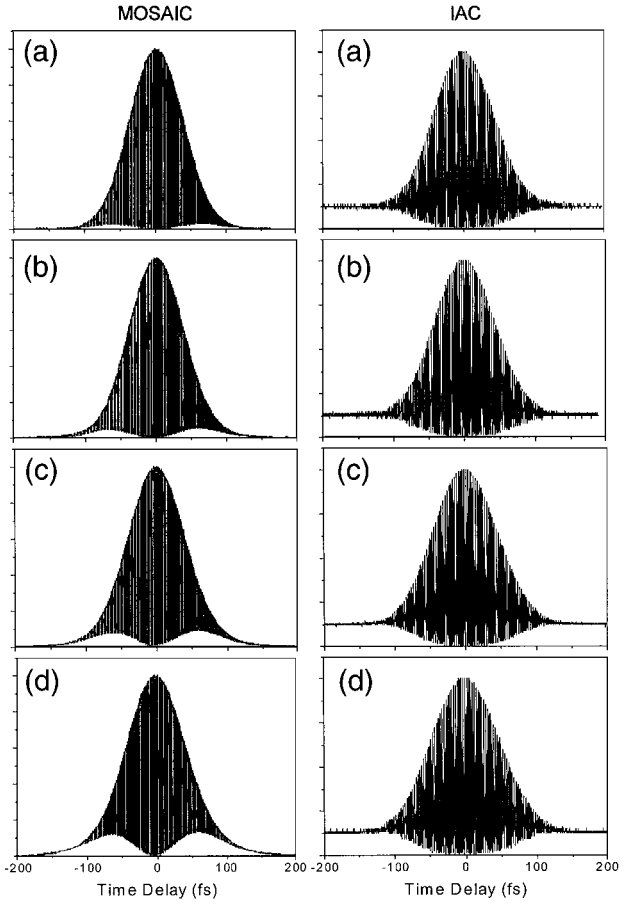

Fig. 2. Measured IAC and the corresponding MOSAIC traces for a cw mode-locked Ti:sapphire laser. We varied the chirp of the pulses by causing the laser beam to propagate through a 6-mm-thick SiO_2 window for (a) zero, (b) two, (c) three, and (d) five passes.

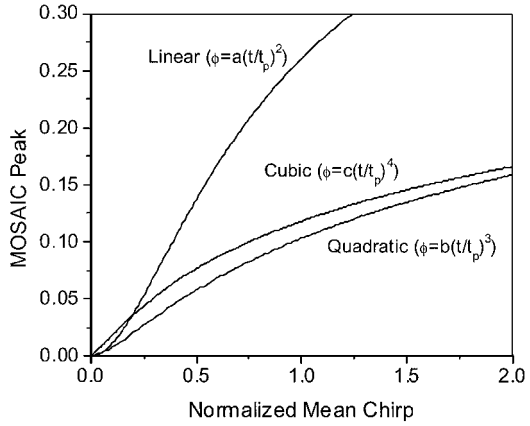

Fig. 3. Calculated MOSAIC peak as a function of the normalized mean chirp for different orders of chirp.

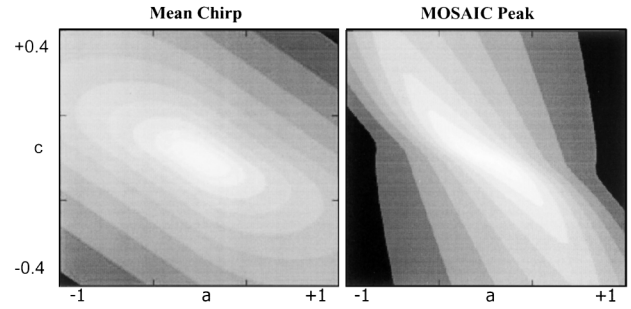

Fig. 4. Contour plots depicting mean chirp (left) and the corresponding MOSAIC peak (right) as the first- and third-order chirps (i.e., a and c parameters) vary in sign and magnitude.

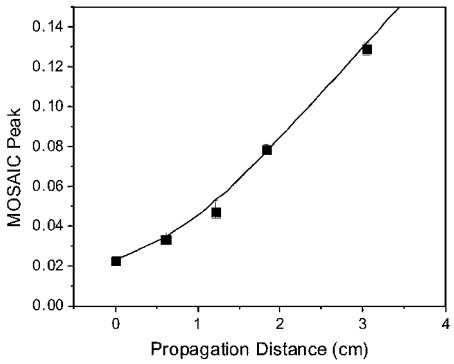

Fig. 5. MOSAIC peak corresponding to the data in Fig. 2 plotted versus the propagation distance in SiO_2. We calculated the solid curve by using the known dispersion for SiO_2 and assuming an initial chirp for the laser pulse, using $a = 0$, $|b| = 0.08(\pm 0.02)$, and $c = 0.024(\pm 0.003)$.

third-order chirp parameters (i.e., a and c coefficients) vary in sign and magnitude. We note that the minima of both graphs (light-shaded central regions) are strongly correlated. This demonstrates that the smallest MOSAIC peak still corresponds closely to the lowest mean chirp in the pulse, even with multiple orders of chirp present. The MOSAIC peaks of the experimental results depicted in Fig. 2 are plotted in Fig. 5 as a function of propagation distance in the fused silica. Also shown is the calculated result from the dispersion data of fused silica. We see that the pulses that exist in the laser are slightly chirped, as evidenced by the nonzero MOSAIC peak. Note that the IAC traces reveal no evidence of chirp. The residual chirp, which we could not eliminate by tuning the prism pair in the oscillator cavity, is due to a small amount of uncompensated third- and fourth-order dispersion. This is verified in the calculated result (Fig. 5) that fits the data assuming $a = 0$, $|b| = 0.08(\pm 0.02)$, and $c = 0.024(\pm 0.003)$ for our 60-fs (FWHM) pulses.

The smallest detectable chirp depends on a given experimental signal-to-noise ratio, provided that the initial autocorrelation signal is purely second order. We investigated the effects of small deviations from quadratic response (e.g., caused by two-photon detector or second-harmonic generation saturation) by considering an intensity response function $I^{2+\epsilon}$ with $-0.4 \leq \epsilon \leq 0.4$ denoting the deviation. Starting with a clean (unchirped) pulse, calculations show that such a deviation causes a distortion in the flatness of the MOSAIC peak by a relatively small magnitude, $\approx -\epsilon/6$ centered at $\tau = 0$. Calculations also indicate that, for the rectangular filter function (described earlier), pulses that contain as few as 1.5 optical cycles (within Δt_{FWHM}) can be accurately analyzed, provided that the mean chirp is ≤ 1.

In conclusion, we have presented a simple, real-time chirp diagnostic for ultrashort laser pulses. This technique, the MOSAIC, is based on a modified-spectrum interferometric autocorrelation measurement. Although we have emphasized the real-time implementation of this technique, we believe it is good practice to convert all the IAC signals to MOSAIC waveforms. This allows a more accurate characterization of the spectral purity of ultrashort pulses.

The support provided through National Science Foundation awards MPS-9977542 and ECS-0100636 is gratefully acknowledged. The authors also thank M. P. Hasselbeck for useful discussions and for proofreading the manuscript. M. Sheik-Bahae's e-mail address is msb@unm.edu.

References

1. J. L. A. Chilla and O. E. Martinez, Opt. Lett. **16,** 39 (1991).
2. D. J. Kane and R. Trebino, IEEE J. Quantum Electron. **29,** 571 (1993).
3. C. Iaconis and I. A. Walmsley, Opt. Lett. **23,** 792 (1998).
4. J. W. Nicholson, J. Jasapara, W. Rudolph, F. G. Omenetto, and A. J. Taylor, Opt. Lett. **24,** 1774 (1999).
5. J. C. M. Diels, J. J. Fontaine, I. C. McMichael, and F. Simoni, Appl. Opt. **24,** 1270 (1985).
6. J.-C. Diels and W. Rudolph, *Ultrashort Laser Pulse Phenomena: Fundamentals, Techniques and Applications on a Femtosecond Time Scale* (Academic, San Diego, Calif., 1996).
7. M. Sheik-Bahae, Opt. Lett. **22,** 399 (1997).
8. L. Sarger, P. Segonds, L. Canioni, F. Adamietz, A. Ducasse, C. Duchesne, E. Fargin, R. Olazcuaga, and G. Leflem, J. Opt. Soc. Am. B **11,** 995 (1994).
9. D. T. Reid, W. Sibbett, J. M. Dudley, L. P. Barry, B. Thomsen, and J. D. Harvey, Appl. Opt. **37,** 8142 (1998).
10. M. V. Klein and T. E. Furtak, *Optics*, 2nd ed. (Wiley, New York, 1986).